A simulated lagged response of the North Atlantic Oscillation to the solar cycle over the period 1960–2009

You may also be interested in:

The impact of a future solar minimum on climate change projections in the Northern Hemisphere
G Chiodo, R García-Herrera, N Calvo et al.

Effects of stratospheric variability on El Niño teleconnections
J H Richter, C Deser and L Sun

Solar cycle modulation of the Pacific–North American teleconnection influence on North American winter climate
Zhongfang Liu, Kei Yoshimura, Nikolaus H Buenning et al.

What is the current state of scientific knowledge with regard to seasonal and decadalforecasting?
Doug M Smith, Adam A Scaife and Ben P Kirtman

A connection from Arctic stratospheric ozone to El Niño-southern oscillation
Fei Xie, Jianping Li, Wenshou Tian et al.

Nonlinear winter atmospheric circulation response to Arctic sea ice concentration anomalies for different periods during 1966–2012
V A Semenov and M Latif

Forcing of the wintertime atmospheric circulation by the multidecadal fluctuations of the North Atlantic ocean
Yannick Peings and Gudrun Magnusdottir

Influence of the Gulf Stream on the Barents Sea ice retreat and Eurasian coldness during early winter
Kazutoshi Sato, Jun Inoue and Masahiro Watanabe

Environmental Research Letters

LETTER

A simulated lagged response of the North Atlantic Oscillation to the solar cycle over the period 1960–2009

M B Andrews[1], J R Knight[1] and L J Gray[2]

[1] Hadley Centre, Met Office, Exeter, EX1 3PB, UK
[2] NCAS-Climate, Department of Physics, Oxford University, Oxford, UK

E-mail: martin.andrews@metoffice.gov.uk

Abstract

Numerous studies have suggested an impact of the 11 year solar cycle on the winter North Atlantic Oscillation (NAO), with an increased tendency for positive (negative) NAO signals to occur at maxima (minima) of the solar cycle. Climate models have successfully reproduced this solar cycle modulation of the NAO, although the magnitude of the effect is often considerably weaker than implied by observations. A leading candidate for the mechanism of solar influence is via the impact of ultraviolet radiation variability on heating rates in the tropical upper stratosphere, and consequently on the meridional temperature gradient and zonal winds. Model simulations show a zonal mean wind anomaly that migrates polewards and downwards through wave–mean flow interaction. On reaching the troposphere this produces a response similar to the winter NAO. Recent analyses of observations have shown that solar cycle–NAO link becomes clearer approximately three years after solar maximum and minimum. Previous modelling studies have been unable to reproduce a lagged response of the observed magnitude. In this study, the impact of solar cycle on the NAO is investigated using an atmosphere–ocean coupled climate model. Simulations that include climate forcings are performed over the period 1960–2009 for two solar forcing scenarios: constant solar irradiance, and time-varying solar irradiance. We show that the model produces significant NAO responses peaking several years after extrema of the solar cycle, persisting even when the solar forcing becomes neutral. This confirms suggestions of a further component to the solar influence on the NAO beyond direct atmospheric heating and its dynamical response. Analysis of simulated upper ocean temperature anomalies confirms that the North Atlantic Ocean provides the memory of the solar forcing required to produce the lagged NAO response. These results have implications for improving skill in decadal predictions of the European and North American winter climate.

1. Introduction

The variability of the Sun's output influences the heating of the stratosphere via the absorption of ultraviolet (UV) by ozone (Haigh 1994, Gray *et al* 2009). Observational studies of the influence of the 11 year solar cycle show warm temperature anomalies in the equatorial upper stratosphere at solar maximum compared to solar minimum (Frame and Gray 2010, Mitchell *et al* 2014). Significant changes in the extratropical atmospheric circulation have been linked to these temperature anomalies (Kodera 1995, Kodera and Kuroda 2002),

and this is supported by modelling studies (e.g. Matthes *et al* 2004, 2006, Ineson *et al* 2011). One of the mechanisms for 'top-down' solar influence (Gray *et al* 2010) involves equatorial stratospheric warm anomalies at solar maximum which increases the mean meridional temperature gradient, resulting in an increase in the mean Westerly wind in the mid-latitude stratosphere. This positive zonal wind anomaly is then amplified by forcing from planetary waves propagating upwards from the troposphere. Along with meridional advection, this wave feedback causes the poleward and downward migration and amplification of the wind

anomaly to the mid- and high-latitude lower strato-sphere, where it is able to influence tropospheric circulation. The resulting surface response involves sea-level pressure changes at solar maximum which are very similar to the positive phase of the Arctic Oscillation (AO), with anomalous low pressure over the North Pole bordered by anomalous high pressure in mid-latitudes (Thompson and Wallace 1998). Conversely, at solar minimum, a negative AO response results from reduced stratospheric meridional temperature gradients and the downward and poleward propagation of negative zonal wind anomalies. This top-down mechanism occurs on seasonal timescales since planetary wave propagation in the stratosphere is limited to the winter half-year.

This 'top-down' mechanism cannot explain the recently identified lag of approximately 3 years between solar maximum (minimum) and an increased tendency of a positive (negative) North Atlantic Oscillation (NAO) signal superimposed on the intrinsic year-to-year NAO variability (Gray *et al* 2013). The ability of the climate system to pro-duce a multi-year lag in the winter NAO response necessitates the persistence of solar signals within the climate system from one winter to the next. Scaife *et al* (2013) showed that the North Atlantic Ocean is a prime candidate for the source of the lag. Model simu-lations have demonstrated that the sub-surface North Atlantic Ocean can be influenced by NAO changes related to the internal variability of stratospheric cir-culation (Reichler *et al* 2012) and changes in multi-decadal solar irradiance (Menary and Scaife 2014). On interannual timescales, Scaife *et al* (2013) presented a mechanism involving coupled atmosphere–ocean feedbacks. The NAO is known to be correlated with a tripole pattern in the North Atlantic sea-surface tem-peratures (SST), (Visbeck *et al* 2003), which extends below the surface into the ocean mixed layer. Due to the seasonal cycle in surface heat and turbulent fluxes, the mixed-layer-depth (MLD) is deeper in winter than in summer. This suggests that a winter sub-surface ocean signal, linked to solar variability, could persist by being isolated underneath the shallower summer mixed layer from the modifying influence of surface fluxes from the atmosphere. In autumn, as the sum-mer mixed-layer erodes and the deeper winter mixed layer becomes established, any sub-surface solar signal would reconnect with the surface, giving it the poten-tial to influence the atmosphere. This sequestration and re-emergence of signals from one winter to the next has been shown to operate in other contexts (Alexander *et al* 1999, Timlin *et al* 2002, Deser *et al* 2003, Taws *et al* 2011), and would give rise to a forcing of the NAO by the ocean (Rodwell and Fol-land 2002). Hanawa and Sugimoto (2004) identified several regions of re-emergence including areas of the North Atlantic relevant to this study. Scaife *et al* (2013) argue that a weak solar-related AO/NAO signal could build up over a number of years in the tripole region of the North Atlantic Ocean and feedback onto the

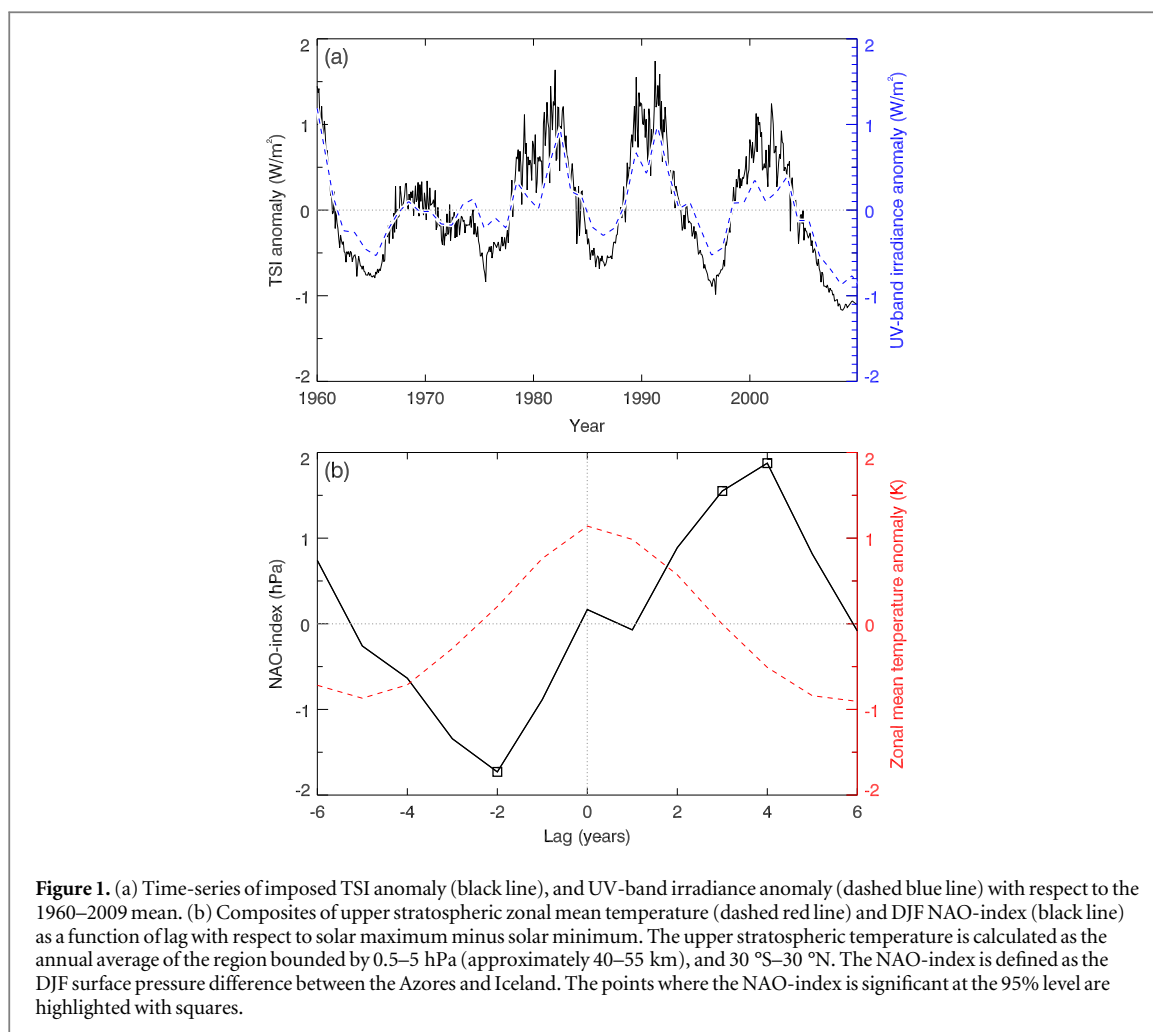atmosphere to produce a peak in the NAO signal after a few years.

Several studies have examined the simulated NAO response to solar forcings. Gray *et al* (2013) and Mitchell *et al* (2015) showed that Coupled Model Intercomparison Project Phase 5 (CMIP5) simula-tions were unable to reproduce the observed NAO response. On the other hand, Ineson *et al* (2011) were able to simulate a realistic amplitude of the NAO response by imposing a higher level of variability in UV-band irradiance. They reproduced the UV-induced 'top-down' mechanism, connecting the upper-stratosphere and the tropospheric NAO. The simulations from Ineson *et al* (2011) were further ana-lysed by Scaife *et al* (2013), who showed that the implied ocean–atmosphere coupling in the model used by Ineson *et al* (2011) was too weak to produce the observed delay.

In this study we use historical simulations of the period 1960–2009 with CMIP5 evolving forcings to explore the influence of solar variability on the NAO. This is different to the experiments of Ineson *et al* (2011) which use constant forcings within their solar maximum and solar minimum scenarios. We use two ensembles, the first with solar irradiance held constant and the second with time-varying spectrally resolved solar variability. The difference in response of the ensembles should reveal the influence of the varying solar cycle on the atmosphere and oceans.

2. Methods

To produce the simulations described in this paper we used the Hadley Centre Global Environmental Model version 3 (HadGEM3, Hewitt *et al* 2011, Walters *et al* 2011). This is an atmosphere–ocean coupled model which includes NEMO v3.2 ocean and CICE sea-ice sub-models. This model is also used by the Met Office Hadley Centre Decadal Prediction System version 2 (DePreSys2) (see Knight *et al* 2014, and references therein). The model atmosphere has a horizontal resolution of 1.25° in latitude by 1.875° in longitude, and 85 vertical levels up to 85 km (~0.1 hPa). This 'high-top' model is capable of simulating stratospheric processes such as UV heating and circulation. The ocean sub-model is a nominal 1° ocean on a tripolar grid with 75 vertical levels. The sea-ice sub-model has four ice thickness categories. The atmosphere and ocean time-steps are 20 and 60 min respectively. Atmosphere–ocean coupling occurs with a frequency of 3 h.

The model has 6 shortwave spectral bands span-ning 0.2–10 μm. The UV band spanning wavelengths 200–320 nm is divided into a further 6 sub-bands to increase sensitivity to the imposed UV variations (Zhong *et al* 2008). Two 12-member ensembles, dif-fering only in solar irradiance forcing, were per-formed, with each member running from 1960 to

Figure 1. (a) Time-series of imposed TSI anomaly (black line), and UV-band irradiance anomaly (dashed blue line) with respect to the 1960–2009 mean. (b) Composites of upper stratospheric zonal mean temperature (dashed red line) and DJF NAO-index (black line) as a function of lag with respect to solar maximum minus solar minimum. The upper stratospheric temperature is calculated as the annual average of the region bounded by 0.5–5 hPa (approximately 40–55 km), and 30 °S–30 °N. The NAO-index is defined as the DJF surface pressure difference between the Azores and Iceland. The points where the NAO-index is significant at the 95% level are highlighted with squares.

2009. The first ensemble has a constant irradiance in each band and is used as a control. The second ensemble has varying 11 year solar cycle irradiance (Lean 2009) with the UV-band irradiance modified to reflect UV variations observed by the Spectral Irradiance Monitor (SIM) instrument on the Solar Radiation and Climate Experiment (SORCE) satellite (Harder *et al* 2009). These UV measurements do not span a complete solar cycle, so a regression with open solar flux (Lockwood *et al* 2004) over the available SIM data period is used to construct a UV-band irradiance timeseries using the open solar flux over the period 1960–2009. We note that the magnitude of solar cycle UV variability remains uncertain, and the variability in the SORCE dataset is likely to be an upper limit (Ermolli *et al* 2013). Figure 1(a) shows the evolution of the total solar irradiance (TSI) variability, together with the irradiance contribution from the modified UV-band.

All other climate forcings were specified using data from CMIP5 historical (up to 2005) and Representative Concentration Pathway 8.5 (beyond 2005) (Jones *et al* 2011). Stratospheric ozone is prescribed on the latitude-height grid as a historical monthly-varying zonal mean, and is based on the SPARC (Stratospheric Processes and their Role in Climate) dataset (Cionni

et al 2011). This includes an estimate of the effect of the solar cycle on stratospheric ozone concentrations, which is present in both ensembles. Responses to ozone variations are not expected to influence the results, therefore, since the solar response will be identified as the difference between ensembles. Consequently, we do not evaluate possible dynamical responses to changes in ozone related to solar variability, although the calculation of stratospheric heating from the imposed solar UV uses the model's specified ozone concentrations. Realistic treatment of the effects of solar cycle ozone changes likely requires fully interactive chemistry–climate simulations and is therefore beyond the scope of this paper.

Each ensemble was initialized using the same initial conditions generated by a control simulation of HadGEM3 with 1960s forcings. Ensemble spread is achieved using a combination of three different initial conditions (separated by ten years in the control simulation) and the Stochastic Kinetic Energy Backscatter (SKEB2) scheme (Tennant *et al* 2011) which applies small stochastically-generated wind increments at every atmospheric model time step. SKEB2 is used to introduce random changes to the model's atmospheric evolution via the selection of different initial 'seed' values.

We define the years of solar maximum and minimum as the upper and lower terciles of the Lean (2009) TSI over the period 1960–2009. This produces 17 solar maximum years (1960, 1969–70, 1978–82, 1989–92, 1999–2003) and 17 solar minimum years (1962–65, 1974–76, 1985–87, 1995–97, 2006–09). The examination of lagged responses can result in slightly fewer years being available for composites when some of the lagged years fall outside the period of our simulations. The average number of solar minimum years for all lags considered in this paper (from −6 to +6 years) is 14 (amounting to 168 ensemble member years) and for solar maximum, 16 (192 ensemble member years). The use of terciles to identify solar maximum and solar minimum years produces blocks of years that are, on average, over 3 years in duration. While this provides better statistical inferences by increasing the effective sample size, the specific phases of the solar cycle associated with particular signals are less well defined.

The influence of the solar forcing is identified as the difference between the means of the control and perturbation ensembles. The advantage of this approach is that we isolate the signal of solar forcing from those of other forcings. Composites for the annual average or December–January–February (DJF) average are then computed for the solar maximum and minimum years. Lagged composites are formed using the equivalent years offset by −6 to +6 years. A Monte-Carlo approach is adopted to calculate two-sided significance at the 95 and 99% levels for the mean-sea-level-pressure (MSLP) fields. To account for autocorrelation between consecutive years within the blocks of solar maximum and solar minimum years, our Monte-Carlo approach produces composites from randomly selected non-overlapping blocks of years from the 1960–2009 dataset. 1000 randomly generated composites of pseudo-maximum and pseudo-minimum years are used to produce the distribution of differences expected by chance, against which the real solar maximum and minimum composites are compared.

3. Results

The annually averaged imprint of solar UV heating on the tropical and sub-tropical upper stratosphere during the solar cycle is readily seen in the lag plot of figure 1(b). The UV-induced warming in the upper stratosphere for solar maximum minus solar minimum peaks at zero lag and results in an annually averaged temperature difference exceeding 1 K, in reasonable agreement with reanalyses (Mitchell *et al* 2015). As the lag increases from 0 to 2 years, the warm anomaly reduces in amplitude before reversing in sign from lag 3 years onwards due to the transition to the opposite phase of the solar cycle.

Unsurprisingly, the simulated tropical upper stratospheric temperature changes resulting from the solar cycle are similar to those found in the HadGEM3 experiments performed by Ineson *et al* (2011). In those experiments, the annual average tropical upper stratospheric temperature difference between solar maximum and solar minimum was about 2 K. This slightly higher value reflects the fact that the differential UV forcing they used (1.2 W m^{-2}) was an extrapolation of observational data to cover the descending phase of the relatively large-amplitude solar cycle 23 (2000–2008). In contrast, the 1960–2009 period examined here includes less pronounced variability in some periods (see figure 1(a)), resulting in a smaller mean solar maximum minus minimum UV change (0.75 W m^{-2}). Taking the difference in mean forcing into account, the upper stratospheric temperature response is almost identical to that found in Ineson *et al* (2011).

Following Ineson *et al* (2011) we look for a surface climate response to the upper stratospheric temperature anomaly. The DJF NAO-index response plotted as a function of lag is shown in figure 1(b). We find that there is only a small solar forcing response in the model NAO in the extreme phase of the solar cycle. Instead we see a statistically significant positive response peaking 3–4 years after solar maximum at the 95% level. Additionally, peak negative NAO responses occur 2 years prior to solar maximum, or approximately 3–4 years after solar minimum. The maximum amplitude of the lagged NAO response is 1.8 hPa. This is consistent with the model response (2.4 hPa) of Ineson *et al* (2011) especially considering the difference in mean forcing. It is smaller, however, than assessed from observations: Ineson *et al* (2011) cite a value of 4.6 hPa based on reanalysis data, while Gray *et al* (2013) show variability of about 3 hPa in the Southern node of the NAO alone. Given that all of these estimates are a sizeable fraction of the observed (7.8 hPa) (HadSLP2; Allan and Ansell 2006) and model (7.7 hPa) interannual DJF standard deviation, they are sufficient to lead to significant surface climate impacts.
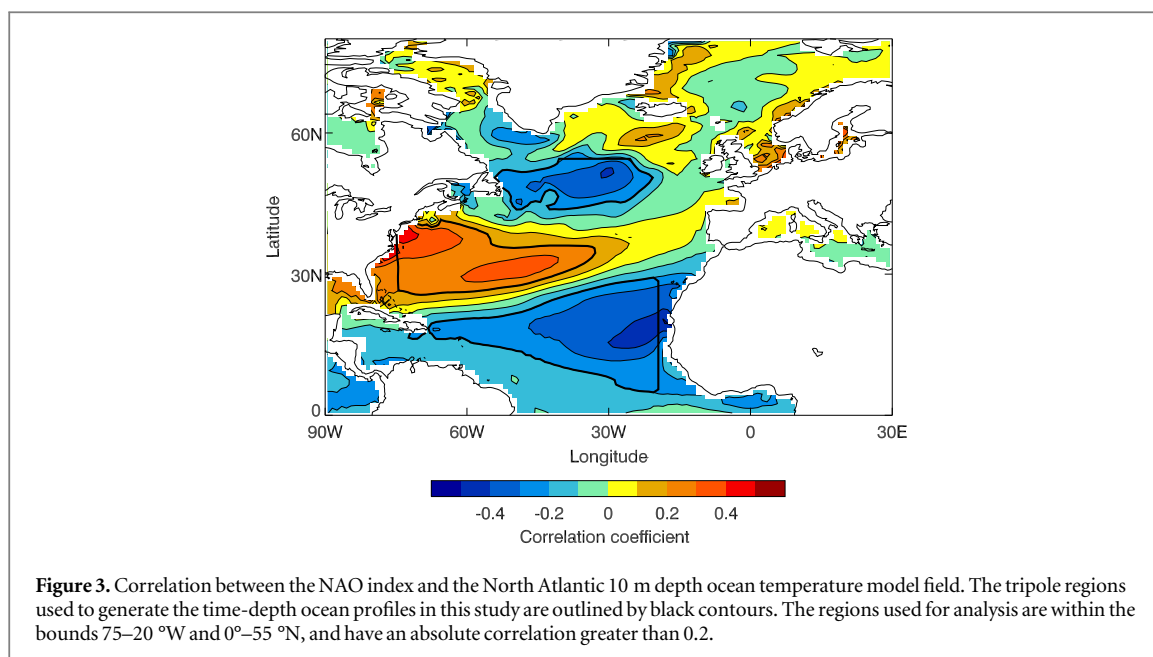
The difference in the composite Northern Hemisphere winter MSLP between the solar variability ensemble and control ensemble for lags of up to 4 years after the peak of the solar cycle is shown in figure 2. At lag 0 years there is a significant positive pressure anomaly in the Aleutian Low region, and a significant negative anomaly over the Arctic extending across Greenland, both of which project onto a positive AO pattern. The Aleutian anomaly is a key feature that occurs in observational analyses (van Loon *et al* 2007) and model experiments in the response to the solar cycle (see, for example, Meehl *et al* 2008, 2009, Roy and Haigh 2010, Gray *et al* 2013, Hood *et al* 2013) and was reproduced in the model experiment of Ineson *et al* (2011). The Aleutian response weakens at lags of 1 year and longer and becomes statistically insignificant.
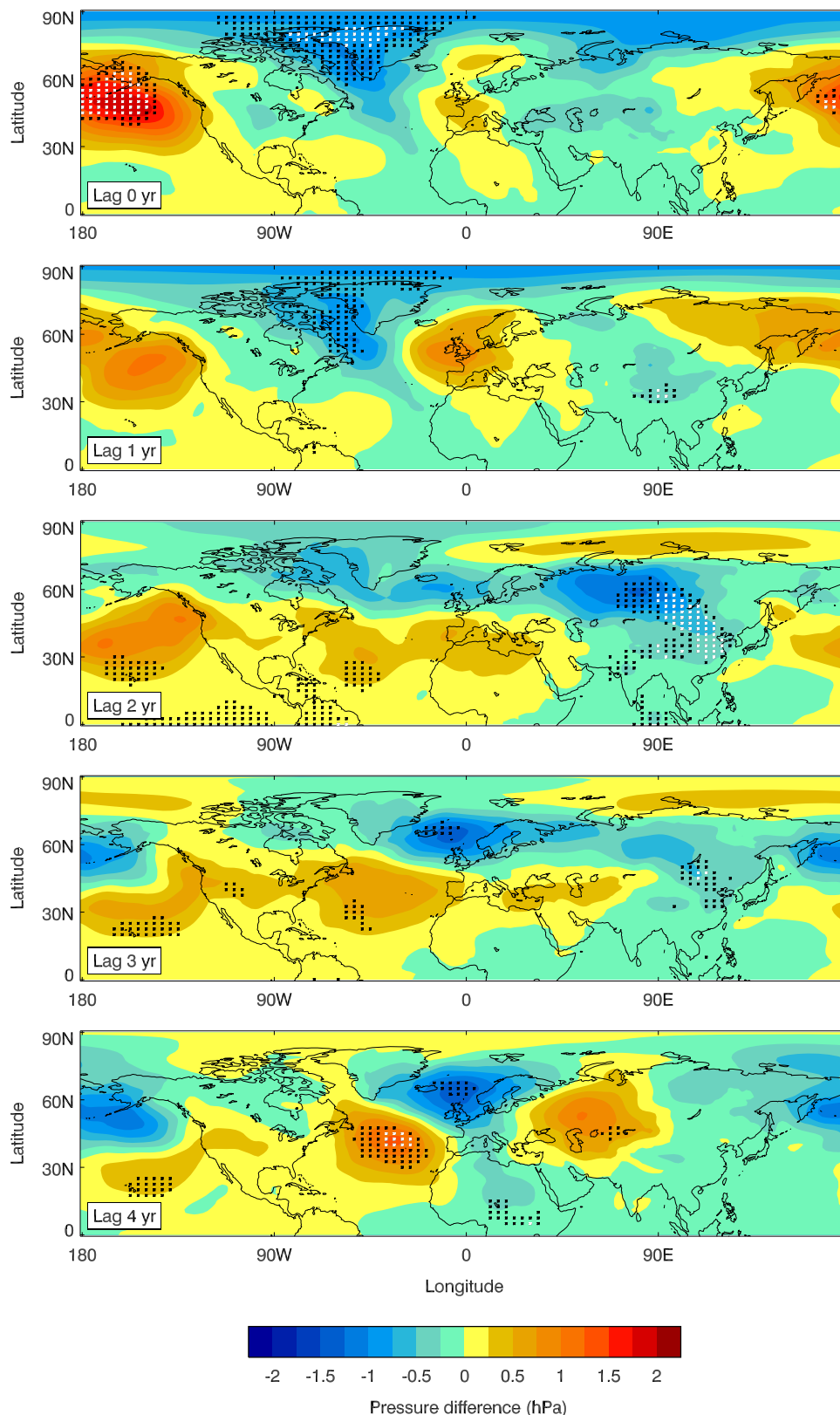
Figure 2. Model response of the DJF Northern Hemisphere MSLP for lags of 0–4 years with respect to solar maximum minus solar minimum. Regions significant at the 95 and 99% confidence level are marked with black and white stippling, respectively.

At a lag of 2 years, the positive AO circulation characterized by negative MSLP anomalies over the Arctic and Greenland diminishes and becomes insignificant. At the same time, dipole MSLP anomalies begin to build in an approximate zonal band in the Northern mid-latitudes, with negative anomalies over Northern Eurasia and positive anomalies over the Pacific and North Atlantic, although local significance is only

Figure 3. Correlation between the NAO index and the North Atlantic 10 m depth ocean temperature model field. The tripole regions used to generate the time-depth ocean profiles in this study are outlined by black contours. The regions used for analysis are within the bounds 75–20 °W and 0°–55 °N, and have an absolute correlation greater than 0.2.

attained for part of this pattern. By 3 years after solar maximum, a positive NAO-like pattern has developed, with positive MSLP anomalies in the Azores High region and significant negative anomalies over the Icelandic region. These centres show significant responses at a lag of 4 years, retaining a strong positive NAO-like character. The results are very similar to those obtained from the observational analysis of Gray *et al* (2013) which shows a statistically significant response in the Azores region only at lags of 1–4 years after a solar maximum.
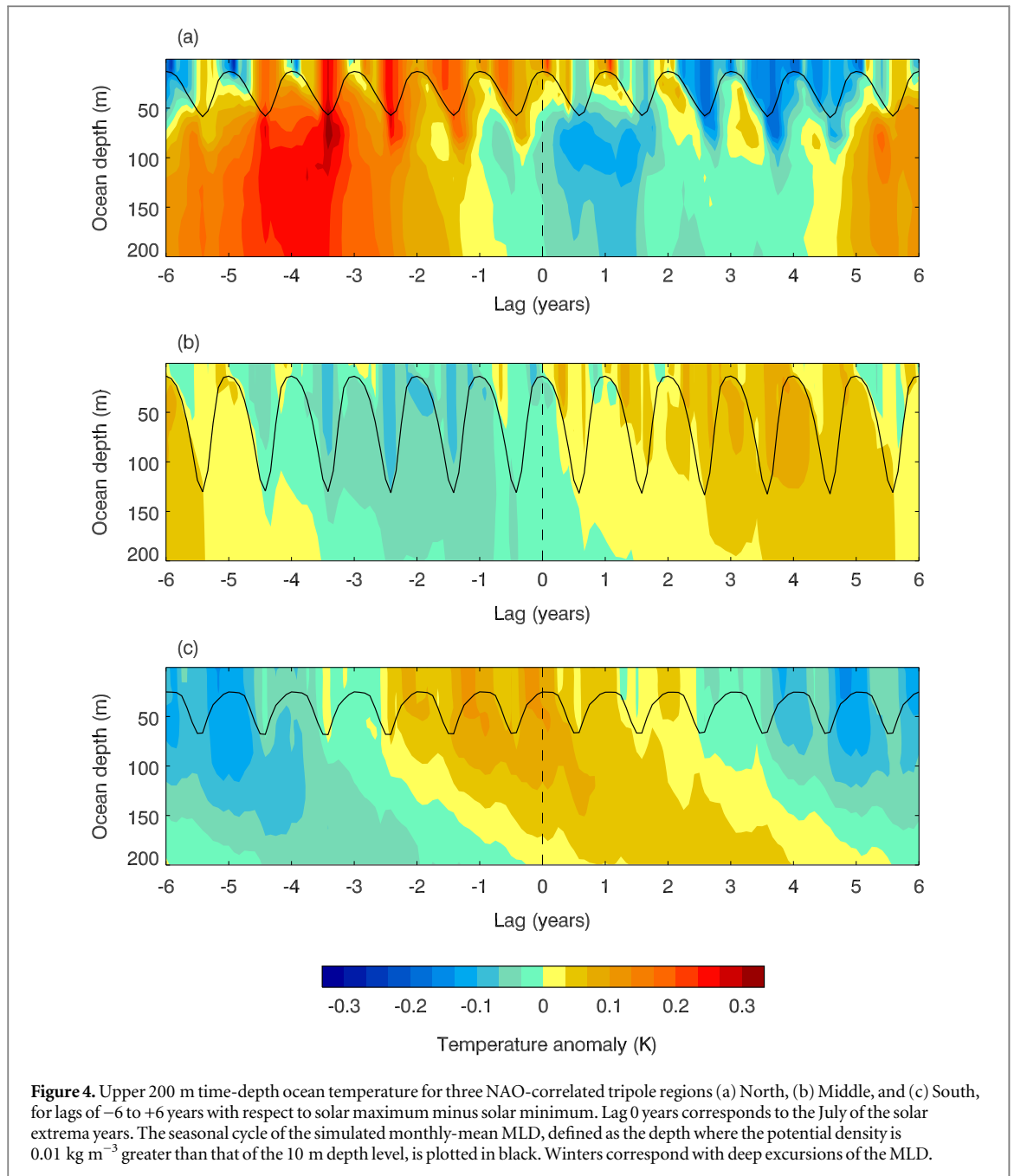
While the simulation of significant responses of the NAO to the solar cycle at lags of 3–4 years agrees with observations, the source of this signal is unclear, since by this point the solar cycle has reached a neutral phase and is beginning to reverse. As a result, the upper stratospheric heating has decreased and also is beginning to reverse (figure 1(b)), so there is no longer a driver for the 'top-down' mechanism. The implication is that a signal of the solar cycle persists somewhere within the climate system and this produces the delayed response in the NAO. The atmosphere generally lacks long-term memory, however, as discussed above, the North Atlantic Ocean may contribute to a lagged response. Here we examine the simulated response of upper ocean temperatures in the North Atlantic to the solar cycle in our experiments.

The NAO is associated with a tripole pattern of SST anomalies in the North Atlantic Ocean (Visbeck *et al* 2003). The spatial configuration of the simulated North Atlantic SST tripole depends to a degree on the model in question, in particular the representation of the North Atlantic storm-track. As a result, we estimate the tripole in HadGEM3 by calculating the correlation between the NAO-index and the 10 m depth ocean temperature for DJF using both ensembles (figure 3). The North Atlantic

tripole pattern in the model has a region of positive correlation with the NAO across the mid-North Atlantic, flanked to the North and South by regions of negative correlation. This pattern is very similar to that found in the observational analysis of Visbeck *et al* (2003), with the exception that the Northern part of the simulated tripole does not extend North of about 55 °N. Peak correlations are of similar magnitude, greater than 0.3 in the central node, and about −0.4 in the Northern and Southern nodes. Tripole temperature anomalies also extend into the sub-surface layers, remaining coherent to depths in excess of 60 m. Composites of sub-surface ocean temperature anomalies for each of the three component regions of the tripole are computed as area-averages of ocean gridpoints where the absolute correlation of the NAO-index with SST is greater than 0.2. We limit the Northern region to 55 °N to avoid the less coherent regions near Greenland which can have sea-ice in winter (Knight *et al* 2014).

Composite solar maximum minus minimum ocean temperature differences for the three North Atlantic tripole regions (referred to as North, Middle and South for convenience) are shown in figure 4 for lags from −6 to +6 years. The simulated monthly average MLD shows seasonal dependence in which the summer MLD is shallow compared to the winter MLD as a result of different insolation and turbulent flux regimes in each season. Seasonal MLD variations remain very similar for both solar maximum and solar minimum years.

Examination of the Middle region (figure 4(b)) shows that the mean temperature at the surface and in the upper layers of the ocean is lagged with respect to the solar cycle in a similar way to the NAO. Predominantly cold anomalies are found in the 5 years leading up to solar maximum, and warm anomalies in

Figure 4. Upper 200 m time-depth ocean temperature for three NAO-correlated tripole regions (a) North, (b) Middle, and (c) South, for lags of −6 to +6 years with respect to solar maximum minus solar minimum. Lag 0 years corresponds to the July of the solar extrema years. The seasonal cycle of the simulated monthly-mean MLD, defined as the depth where the potential density is 0.01 kg m^{-3} greater than that of the 10 m depth level, is plotted in black. Winters correspond with deep excursions of the MLD.

the 5 years following solar maximum. The positive near-surface temperature anomaly occurring in the first winter (which is identified by the first deep excursion of the MLD after lag 0 years) is consistent with a positive AO response to the 'top-down' atmospheric mechanism. Part of this signal persists under the shallow summer mixed layer until the following winter. A larger warm signal is then seen in the second winter compared to the first winter. We suggest that this gain is attributable to the residual warmth from the first winter, since the water below the summer thermocline is entrained into the mixed layer as the MLD deepens in autumn. This is superimposed onto the direct effect of solar forcing of the atmosphere in the second winter as a result of the continued influence of the 'top-down' mechanism.

The solar signal grows in subsequent winters as storage of heat below the summer mixed layer also increases, peaking in the fourth winter. As surface temperature in this region can drive the NAO, this implies a positive feedback causing the winter NAO signal to be amplified over the course of a few years. In turn, the strengthened NAO signal amplifies the tripole SST anomalies. The accumulation of sub-surface warmth declines after year 4 (approximately ¼ cycle), as by this point in the solar cycle the transition to stratospheric cooling drives an opposing NAO tendency, eroding the positive ocean temperature and NAO anomalies.

The composite temperature anomalies for the North tripole region (figure 4(a)) show the opposite phasing to those in the middle region, with warm

ocean temperature anomalies prior to solar maximum and an overall tendency for cool anomalies following solar maximum. Although the monthly-averaged MLD appears shallow in this region, in fact, strong surface buoyancy forcing leads to short-lived episodes of very deep mixing, explaining the apparent penetration of winter temperature anomalies below the MLD. Evidence for seasonal re-emergence in this region is weak, however, as summer anomalies below the mixed layer often appear to be of opposite sign to those in the preceding winter (e.g. at 2–3 year lag). The explanation for this is that this region has strong depth-dependent horizontal transport of anomalies, which disrupts the vertical coherence implicitly required for the re-emergence mechanism. For example, the negative temperature anomaly centred at a depth of approximately 80 m at lag 0 years is due to an earlier cool signal transported into the region from the Labrador Sea (not shown). As a result, the composite winter anomalies seen in the North region are more likely to be a passive response to solar-driven NAO changes than an active part of the feedback mechanism.

The South tripole region (figure 4(c)) does not demonstrate the same lagged response as the other two regions. Instead, surface and mixed-layer anomalies appear synchronised with the solar cycle, with the transition from warm to cool winter anomalies emerging after a lag of two years. It appears that the South region responds directly to the change in surface insolation, with an increase in the ocean heat content around solar maximum and a decrease around solar minimum.

The results suggest that only the Middle region exhibits the crucial re-emergence mechanism that provides the necessary feedback to produce a lagged solar influence on the NAO. The North region does not appear to play an active role due to differential horizontal transport in the water column disrupting the seasonal re-emergence mechanism. The solar signal in the South region is not coherent with the other tripole regions due to solar influences that are unrelated to the 'top-down' mechanism and its effects on the ocean.

The ocean interaction with the NAO highlighted in these experiments is not specific to NAO responses to solar variability. The results, therefore, are relevant in the wider context of winter ocean–atmosphere coupling. They reveal that the Middle region is likely to be a principal source of re-emergence feedback while the North region is unlikely to have a similar influence due to regional oceanic circulation. The lack of coherence of the South region with the NAO in our experiments prevents us from making general inferences about its contribution to NAO feedback.

It was shown by Scaife *et al* (2013) that a simple mechanistic model fitted to the results of the experiments of Ineson *et al* (2011) produced a lag of 1–2 years, and that stronger ocean–atmosphere coupling would be needed to reproduce the 3–4 year lag

exhibited by both observational analyses and this study. The application of a constant instead of time-varying solar irradiance in their experiments may account for this difference, although identifying exactly how this difference arises would require substantial further investigation.

4. Summary

We have investigated the NAO response to solar variability using a state-of-the-art atmosphere–ocean coupled model. Historical ensembles for the period 1960–2009 were performed with constant and time-varying solar irradiance. Analysis of the differences between the ensembles was performed to identify solar cycle responses in the atmosphere and ocean. The results demonstrate tropical upper stratospheric heating in response to the imposed UV change at solar maximum compared to solar minimum, and confirm the results of Ineson *et al* (2011), showing a subsequent surface winter NAO response via a 'top-down' mechanism. The response of the NAO peaks 3–4 years following the extreme phase of the solar cycle. This finding is consistent with a recent re-evaluation of observed responses to the solar cycle (Gray *et al* 2013) which shows the largest NAO signal at a similar lag. The in-phase response of the Aleutian Low is also in agreement with observational analyses.

We diagnose the source of the NAO lag in the model by examining its surface and sub-surface solar responses in the North Atlantic Ocean. We find evidence for amplification of 'top-down' solar-related NAO changes via an ocean feedback over a period of several years, as suggested by Scaife *et al* (2013). This feedback is analysed by examining solar cycle responses in the different nodes of the North Atlantic tripole SST pattern, as this pattern reflects NAO–ocean coupling. The Northern and Middle nodes of the tripole show temperature responses in the surface and sub-subsurface ocean with a similar lag to the NAO. The Southern node, however, does not show any lag. In the Middle node we find re-emergence of solar signals imprinted on the ocean from the previous winter. By remaining intact below the shallow ocean mixed-layer that forms in summer, these signals can re-emerge in winter and reinforce the 'top-down' forcing of the NAO via coupling with the atmosphere. This mechanism is not evident in the Northern and Southern nodes. The simulated re-emergence in the North Atlantic Ocean causes an accumulation of the solar signal, allowing the NAO to grow over several years. This growth is limited by the reversal of the solar cycle, resulting in a lag approximately equal to one quarter of its period. Although we do not explicitly demonstrate here that the growth in the NAO response arises through feedback from the solar SST signal in the Middle node the existence of this feedback is supported by previous studies (Rodwell and Folland 2002,

Timlin *et al* 2002) that show the influence of tripole SSTs on the NAO.

The NAO (Hurrell *et al* 2003) is a key mode of regional climate variability that strongly influences the wintertime weather of Northern Europe and Eastern North America. The ability to reproduce the lagged NAO response to solar forcing in atmosphere–ocean coupled models offers the possibility of increased NAO predictability and hence skill in seasonal fore-casts (Scaife *et al* 2014) and decadal forecasts up to a few years ahead (Smith *et al* 2012).

Acknowledgments

References

Alexander M A, Deser C and Timlin M S 1999 The reemergence of SST anomalies in the North Pacific Ocean *J. Clim.* **12** 2419–33

Allan R and Ansell T 2006 A new globally complete monthly historical gridded mean sea level pressure dataset (HadSLP2): 1850–2004 *J. Clim.* **19** 5816–42

Cionni I, Eyring V, Lamarque J F, Randel W J, Stevenson D S, Wu F, Bodeker G E, Shepherd T G, Shindell D T and Waugh D W 2011 Ozone database in support of CMIP5 simulations: results and corresponding radiative forcing *Atmos. Chem. Phys.* **11** 11267–92

Deser C, Alexander M A and Timlin M S 2003 Understanding the persistence of sea surface temperature anomalies in midlatitudes *J. Clim.* **16** 57–72

Ermolli I *et al* 2013 Recent variability of the solar spectral irradiance and its impact on climate modelling *Atmos. Chem. Phys.* **13** 3945–77

Frame T H A and Gray L J 2010 The 11 yr solar cycle in ERA-40 data: an update to 2008 *J. Clim.* **23** 2213–22

Gray L J, Rumbold S T and Shine K P 2009 Stratospheric temperature and radiative forcing response to 11 year solar cycle changes in irradiance and ozone *J. Atmos. Sci.* **66** 2402–17

Gray L J *et al* 2010 Solar influences on climate *Rev. Geophys.* **48** RG4001

Gray L J, Scaife A A, Mitchell D M, Osprey S, Ineson S, Hardiman S, Butchart N, Knight J, Sutton R and Kodera K 2013 A lagged response to the 11 year solar cycle in observed winter Atlantic/European weather patterns *J. Geophys. Res. Atmos.* **118** 13405–20

Haigh J D 1994 The role of stratospheric ozone in modulating the solar radiative forcing of climate *Nature* **370** 554–546

Hanawa K and Sugimoto S 2004 'Reemergence' areas of winter sea surface temperature anomalies in the world's oceans *Geophys. Res. Lett.* **31** L10303

Harder J W, Fontenla J M, Pilewskie P, Richard E C and Woods T N 2009 Trends in solar spectral irradiance variability in the visible and infrared *Geophys. Res. Lett.* **36** L07801

Hewitt H T, Copsey D, Culverwell I D, Harris C M, Hill R S R, Keen A B, McLaren A J and Hunke E C 2011 Design and implementation of the infrastructure of HadGEM3: the next-generation Met Office climate modelling system *Geosci. Model Dev.* **4** 223–53

Hood L, Schimanke S, Spangehl T, Bal S and Cubasch U 2013 The surface climate response to 11 yr solar forcing during Northern winter: observational analasyes and comparisons with GCM simulations *J. Clim.* **26** 7489–506

Hurrell J W, Kushnir Y, Ottersen G and Visbeck M 2003 The North Atlantic Oscillation: climate significance and environmental impact *Geophys. Monogr. Ser.* **134** 1–36

Ineson S, Scaife A A, Knight J R, Manners J C, Dunstone N J, Gray L J and Haigh J D 2011 Solar forcing of winter climate variability in the Northern Hemisphere *Nat. Geosci.* **4** 753–7

Jones C D *et al* 2011 The HadGEM2-ES implementation of CMIP5 centennial simulations *Geosci. Model Dev.* **4** 543–70

Knight J R *et al* 2014 Predictions of climate several years ahead using an improved decadal prediction system *J. Clim.* **27** 7550–67

Kodera K 1995 On the origin and nature of the interannual variability of the winter stratospheric circulation in the Northern hemisphere *J. Geophys. Res.* **100** 14077–87

Kodera K and Kuroda Y 2002 Dynamical response to the solar cycle *J. Geophys. Res.* **107** 4749

Lean J L 2009 Available at http://solarisheppa.geomar.de/ solarisheppa/sites/default/files/data/ Calculations_of_Solar_Irradiance.pdf

Lockwood M, Forsyth R B, Balogh A and McComas D J 2004 Open solar flux estimates from near-Earth measurements of the interplanetary magnetic field: comparison of the first two perihelion passes of the Ulysses spacecraft *Ann. Geophys.* **22** 1395–405

Matthes K, Langematz U, Gray L L, Kodera K and Labitzke K 2004 Improved 11 year solar signal in the Freie Univerität Berlin climate middle atmosphere model (FUB-CMAM) *J. Geophys. Res.* **109** D06101

Matthes K, Kuroda Y, Kodera K and Langematz U 2006 Transfer of the solar signal from the stratosphere to the troposphere: Northern winter *J. Geophys. Res.* **111** D06108

Meehl G A, Arblaster J M, Branstator G and van Loon H 2008 A coupled air–sea response mechanism to solar forcing in the pacific region *J. Clim.* **21** 2883–97

Meehl G A, Arblaster J M, Matthes K, Sassi F and van Loon H 2009 Amplifying the pacific climate system response to a small 11 year solar cycle forcing *Science* **325** 1114–8

Menary M B and Scaife A A 2014 Naturally forced multidecadal variability of the Atlantic meridional overturning circulation *Clim. Dyn.* **42** 1347–62

Mitchell D M *et al* 2014 Signatures of naturally induced variability in the atmosphere using multiple reanalysis datasets *Q. J. R. Meterol. Soc.* accepted

Mitchell D M *et al* 2015 Solar signals in CMIP-5 simulations: the stratospheric pathway *Q. J. R. Meterol. Soc.* accepted

Reichler T, Kim J, Manzini E and Kröger J 2012 A stratospheric connection to Atlantic climate variability *Nat. Geosci.* **5** 783–7

Rodwell M J and Folland C K 2002 Atlantic air–sea interaction and seasonal predictability *Q. J. R. Meteorol. Soc.* **128** 1413–43

Roy I and Haigh J D 2010 Solar cycle signals in sea level pressure and sea surface temperature *Atmos. Chem. Phys.* **10** 3147–53

Scaife A A, Ineson S, Knight J R, Gray L, Kodera K and Smith D M 2013 A mechanism for lagged North Atlantic climate response to solar variability *Geophys. Res. Lett.* **40** 434–9

Scaife A A *et al* 2014 Skillful long-range prediction of European and North American winters *Geophys. Res. Lett.* **41** 2514–9

Smith D M, Scaife A A and Kirtman B P 2012 What is the current state of scientific knowledge with regard to seasonal and decadal forecasting? *Environ. Res. Lett.* **7** 015602

Taws S L, Marsh R, Wells N C and Hirschi J 2011 Re-emerging ocean temperature anomalies in late-2010 associated with a repeat negative NAO *Geophys. Res. Lett.* **38** L20601

Tennant W J, Shutts G J, Arribas A and Thompson S A 2011 Using a
    stochastic kinetic energy backscatter scheme to improve
    MOGREPS probabilistic forecast skill *Mon. Weather Rev.* **139**
    1190–206

Timlin M S, Alexander M A and Deser C 2002 On the reemergence
    of North Atlantic SST anomalies *J. Clim.* **15** 2707–12

Thompson D W J and Wallace J M 1998 The Arctic Oscillation
    signature in the wintertime geopotential height and
    temperature fields *Geophys. Res. Lett.* **25** 1297–300

van Loon H, Meehl G A and Shea D J 2007 Coupled air–sea response
    to solar forcing in the Pacific region during Northern winter
    J. Geophys. Res. Atmos. **112** D02108

Visbeck M, Chassignet E P, Curry R G, Delworth T L,
    Dickson R R and Krahmann G 2003 The ocean's response to
    North Atlantic Oscillation variability *The North Atlantic
    Oscillation* ed J Hurrell, Y Kushnir, G Ottersen and
    M Visbeck (Washington, DC: American Geophysical Union)
    (doi:10.1029/134GM06)

Walters D N *et al* 2011 The Met Office unified model global
    atmosphere 3.0/3.1 and JULES global land 3.0/3.1
    configurations *Geosci. Model Dev.* **4** 919–41

Zhong W, Osprey S M, Gray L J and Haigh J D 2008 Influence of the
    prescribed solar spectrum on calculations of atmospheric
    temperature *Geophys. Res. Lett.* **35** L22813